JACS
JOURNAL OF THE AMERICAN CHEMICAL SOCIETY

COMMUNICATION

pubs.acs.org/JACS

Aβ40 and Aβ42 Amyloid Fibrils Exhibit Distinct Molecular Recycling Properties

Laia Sánchez,[†] Sergio Madurga,[‡] Tara Pukala,[§] Marta Vilaseca,[∥] Carmen López-Iglesias,[⊥] Carol V. Robinson,[◇] Ernest Giralt,[*,†,#] and Natàlia Carulla[*,†,¶]

[†]Institute for Research in Biomedicine (IRB Barcelona), Barcelona 08028, Spain

[‡]Department of Physical Chemistry and IQTCUB, University of Barcelona, Barcelona 08028, Spain

[§]School of Chemistry and Physics, University of Adelaide, Adelaide 5005, Australia

[∥]Mass Spectrometry Core Facility, IRB Barcelona, Barcelona, Spain

[⊥]In Situ Molecular Identification Unit, Scientific-Technical Services, University of Barcelona, Barcelona, Spain

[◇]Department of Chemistry, Physical and Theoretical Chemistry Laboratory, University of Oxford, Oxford OX13QZ, United Kingdom

[#]Departament of Organic Chemistry, University of Barcelona, Barcelona, Spain

[¶]ICREA Researcher at IRB Barcelona

Supporting Information

ABSTRACT: A critical aspect to understanding the molecular basis of Alzheimer's disease (AD) is the characterization of the kinetics of interconversion between the different species present during amyloid-β protein (Aβ) aggregation. By monitoring hydrogen/deuterium exchange in Aβ fibrils using electrospray ionization mass spectrometry, we demonstrate that the Aβ molecules comprising the fibril continuously dissociate and reassociate, resulting in molecular recycling within the fibril population. Investigations on Aβ40 and Aβ42 amyloid fibrils reveal that molecules making up Aβ40 fibrils recycle to a much greater extent than those of Aβ42. By examining factors that could influence molecular recycling and by running simulations, we show that the rate constant for dissociation of molecules from the fibril (k_{off}) is much greater for Aβ40 than that for Aβ42. Importantly, the k_{off} values obtained for Aβ40 and Aβ42 reveal that recycling occurs on biologically relevant time scales. These results have implications for understanding the role of Aβ fibrils in neurotoxicity and for designing therapeutic strategies against AD.

Alzheimer's disease (AD) is a progressive neurodegenerative disorder characterized by aggregation of the amyloid-β protein (Aβ) into amyloid fibrils.[1] Aβ fibrils are the principal constituents of the diffuse and neuritic plaques found in regions of the brain affected by the disease. As such, these fibrils were initially thought to be the pathogenic agent in AD.[2] However, little correlation has been found between the amount of plaques in the brain and the severity of AD.[3] Over the past decade, this puzzle has been resolved by emerging data that impute intermediates of the aggregation process, such as Aβ oligomers, as the species responsible for neurodegeneration.[4] However, recent data have shown that fibrillar Aβ plaques are a potential reservoir of oligomeric Aβ species.[5] On one hand, this has reconciled the role of fibrillar Aβ plaques versus Aβ oligomers as the responsible toxic species in AD. On the other hand, it suggests that to understand the basis of AD and the role of Aβ in AD it is crucial to characterize the kinetics of interconversion between the different species present during Aβ aggregation.

Hydrogen−deuterium exchange (H/D) experiments measure the degree of protection of labile hydrogens against exchange with solvent deuterons as a function of time. It is a powerful method for studying the structure, stability, dynamics, and folding of proteins.[6−9] In previous work,[10] we used carefully designed H/D experiments to study amyloid fibrils formed by an SH3 domain of the α-subunit of bovine phosphatidylinositol-3′-kinase (PI3-SH3), a generic model of amyloid formation.[11] We showed that molecules comprising the fibrils continuously dissociate and reassociate, resulting in molecular recycling within the fibril population.[10] We have now extended this work to the explicit study of Aβ amyloid fibrils and show that they also undergo recycling. The ability to observe this dynamic behavior has allowed us to study recycling for Aβ40 and Aβ42 fibrils, variants that are 40 and 42 residues long, which have different roles in AD. Although Aβ40 is the most abundant form, several lines of evidence actually support Aβ42 as being more strongly linked to the etiology of AD.[12] Herein, we report on important differences in the recycling properties of Aβ40 and Aβ42 amyloid fibrils. To determine the origin of said differences, we evaluated the effects of fibril length distribution and fibril morphology and then performed simulation studies. Based on these results, we propose that differences in Aβ40 and Aβ42 recycling stem from differences between each variant's average dissociation rate constant (k_{off}).

We first prepared Aβ40 and Aβ42 fibrils at pH 7.4. Electron micrographs of these samples show that the predominant morphology for the fibrils is a 5-nm wide filament with a slight tendency to laterally associate into bundles (Figure 2a,b). Aβ40 amyloid fibrils were exposed to a deuterated buffer for different periods of time (Figure 1). After different exchange times, fibrils were ultracentrifuged, and the resulting pelleted fibrils were freeze-dried to quench the exchange. Dissolving the pelleted

Received: December 29, 2010
Published: April 12, 2011

dx.doi.org/10.1021/ja1117123 | J. Am. Chem. Soc. 2011, 133, 6505–6508

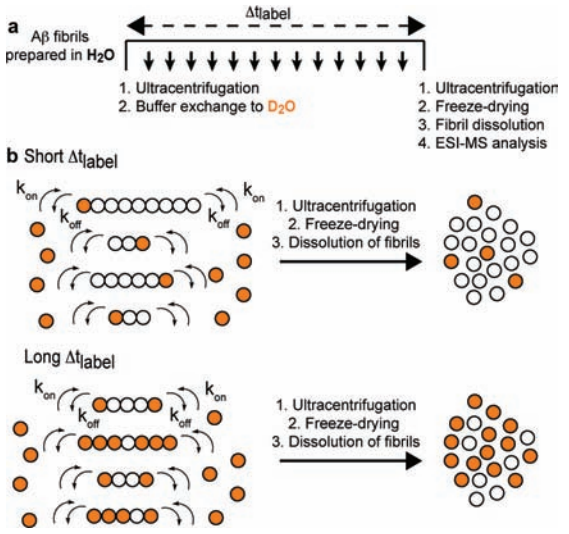

Figure 1. Schematic description of the H/D experiment designed to study molecular recycling within Aβ fibrils. (a) Protonated Aβ fibrils are exposed to deuterated buffer for varying periods of time (Δt_{label}). After the labeling pulse, the solution is ultracentrifuged to remove any soluble protein and the pelleted fibrils are freeze-dried to quench exchange. Amyloid fibrils are later solubilized into monomers by transfer to a DMSO solution and analyzed by ESI-MS. (b) Schematic of the recycling mechanism for a distribution of fibrils at different times of exchange. Molecules dissociate and reassociate through both ends of the fibril. Following fibril dissolution, two populations of molecules are found in solution, those corresponding to the population of molecules that have not yet dissociated from the fibrils (white circles), and those representing the population that have dissociated from the fibrils and subsequently reincorporated after complete exchange (orange circles).

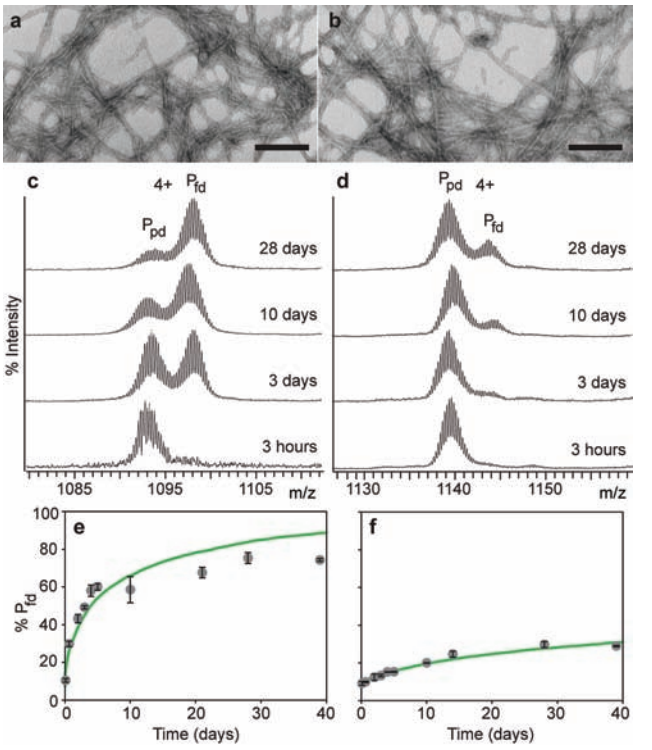

Figure 2. Molecular recycling within Aβ40 and Aβ42 fibrils at pH 7.4. Electron micrographs of (a) Aβ40 fibrils and (b) Aβ42 fibrils, obtained after incubation of either protein in 50 mM ammonium acetate, 1 mM Tris, and 0.01% NaN_3 at pH 7.4 and 25 °C without agitation. The scale bars represent 100 nm. Mass spectra (4+ charge state) showing the relative populations of P_{pd} and P_{fd} species after different times of exchange for (c) Aβ40 and (d) Aβ42. The spectral intensities are all plotted relative to the most intense peak in the spectra. Plot of the relative fraction of P_{fd} molecules in the sample as a function of time of exchange (gray circles) compared to the best fit obtained from the simulations (green curve) for (e) Aβ40, $k_{off} = 0.6\ s^{-1}$ and (f) Aβ42, $k_{off} = 1.0 \times 10^{-2}\ s^{-1}$. The error bars represent the standard deviations resulting from duplicate samples. Standard deviation values smaller than 1 are difficult to observe.

fibrils in a dimethylsulfoxide (DMSO) based buffer efficiently breaks them down into monomers while preserving the exchange information.[7] The deuterium content of the samples was then analyzed by ESI-MS, which has the unique ability to detect and characterize populations of protein molecules with different degrees of exchange.[10,13]

The mass spectra of Aβ40 amyloid fibrils subjected to the aforementioned protocol show two extremely well-resolved peaks (Figure 2c), indicating that the fibrils contain two distinct, isotopically labeled populations of Aβ40. The lower-mass population (P_{pd}, for partially deuterated) corresponds to a population of Aβ40 molecules in which 20.7 ± 0.5 backbone amides had undergone H/D exchange. The higher-mass population (P_{fd}, for fully deuterated) corresponds to species in which 38.6 ± 0.6 backbone amides had undergone H/D exchange. During recycling, and when fibrils are exposed to a deuterated buffer, protein molecules dissociate from the fibril with a rate constant k_{off}. Once in solution, H/D exchange occurs rapidly, with a rate constant k_{ex}. Finally, protein molecules reincorporate into the fibril as fully deuterated species with a rate constant k_{on}. Thus, molecular recycling is consistent with a bimodal isotopic distribution obtained through the EX1 exchange mechanism. After dissociating from the fibrils, molecules are long enough in solution to allow all labile hydrogen atoms to be exchanged before reincorporating back into the fibril. Other H/D experiments designed to probe the core structure of Aβ40 amyloid fibrils have revealed that a set of ~19 amide protons readily exchange with solvent deuterons.[6] This value is very similar to the number of backbone amides that have exchanged in our P_{pd} species (20.6 ± 0.5), suggesting that the P_{pd} species correspond to the population of molecules that had not dissociated from the fibrils (white circles in Figure 1b). The mass of the detected P_{fd} species corresponds to species in which most of the backbone amides have undergone exchange (38.6 ± 0.6, out of 39). This is in agreement with the population of Aβ40 molecules that dissociated from the fibrils, underwent exchange, and then reincorporated into the fibril ensemble (orange circles in Figure 1b). When the fibrils were left to undergo exchange for longer periods of time before MS analysis, the intensity of the P_{fd} species increased relative to that of the P_{pd} species. After 3 days, 49.2 ± 0.8% of the molecules within the fibrils were fully deuterated, and after 39 days, 74.3 ± 0.8% of the molecules appeared as P_{fd} species (Figure 2e).

We then studied Aβ42 fibrils using the aforementioned H/D experiment. The mass spectra of Aβ42 amyloid fibrils exposed to a deuterated buffer for different periods of time also show two well-resolved peaks (Figure 2d). The lower mass population, P_{pd}, represents a population of molecules in which 23.0 ± 0.9 backbone amides underwent exchange. The higher mass population, P_{fd}, corresponds to species in which nearly all of the backbone amides underwent exchange (39.6 ± 1.2, out of 41). Also, as observed for Aβ40 amyloid fibrils, when the Aβ42 fibrils were left to exchange for longer periods of time before ESI-MS

dx.doi.org/10.1021/ja1117123 |J. Am. Chem. Soc. 2011, 133, 6505–6508

analysis, the intensity of the P_{fd} species increased relative to that of the P_{pd} species (Figure 2d). Nevertheless, although Aβ40 and Aβ42 fibrils both undergo recycling, we noticed marked differences in their recycling properties. Molecules comprising Aβ40 fibrils recycle to a much greater extent than those of Aβ42. After 3 days, 49.2 $\pm$ 0.8% of the Aβ40 fibril molecules were fully deuterated, compared to only 13.3 $\pm$ 0.6% for Aβ42; likewise, after 39 days, 74.3 $\pm$ 0.8% of the Aβ40 fibril molecules were fully deuterated, compared to only 28.9 $\pm$ 0.3% for Aβ42 (Figure 2e,f).

One possible explanation for the different recycling properties observed within Aβ40 and Aβ42 amyloid fibrils is differences between their corresponding fibril-length distributions. In previous work,[10] we showed that distributions with shorter fibrils have more fibril ends that can undergo recycling, which leads to a greater extent of deuteration. According to this premise, the differences that we observed for Aβ40 and Aβ42 fibrils would mean that the former, on average, should be considerably shorter than the latter. To test this possibility, we estimated the respective fibril length distributions of Aβ40 and of Aβ42 based on transmission electron microscopy (TEM) images. However, we found that the Aβ40 and Aβ42 fibrils were actually similar in length: in fact, the Aβ40 fibrils were slightly longer than the Aβ42 fibrils (Figure S1). This result is opposite to what one might predict from exchange and indicates that the observed differences in recycling are not due to differences in fibril length.

Another explanation for the different recycling properties observed within Aβ40 and Aβ42 amyloid fibrils is differences in the average dissociation rate constant of molecules from the fibrils, k_{off}, of the two Aβ variants. Analysis of the plot of isotope exchange against time (Figure 2e,f) enables obtaining quantitative estimates of k_{off}, as during recycling the k_{off} limits the appearance of the P_{fd} molecules. We constructed a model considering a fibril ensemble with the same fibril length distribution as obtained from the TEM measurements of fibrils grown at pH 7.4, whereby dissociation and reassociation occur at both ends of the fibril and at the same rate (Figure 1b). We then used it to run various simulations to obtain estimates of the k_{off} value for each Aβ variant. The simulations that best mimicked the experimental time course of the isotope exchange reaction provided the following estimates for k_{off}: 0.6 s^{-1} for Aβ40 (green curve in Figure 2e) and 1.0 $\times$ 10^{-2} s^{-1} for Aβ42 (green curve in Figure 2f) revealing that the k_{off} value for Aβ40 is 60 times larger than that for Aβ42.

Aβ40 and Aβ42 fibrils produced at pH 7.4 comprise a 5-nm wide filament with a slight tendency to laterally associate into bundles (Figure 2a,b). Fibril morphology is sensitive to subtle differences in fibril growth conditions (pH, temperature, buffer composition, and protein concentration).[14] To examine the effect of fibril bundles on the dissociation properties of Aβ molecules from the fibrils, we incubated Aβ40 and Aβ42 separately at pH 2.0 and 37 °C without agitation, conditions reported as leading to few fibril bundles.[15] Study of the resulting fibrils by EM revealed that both Aβ40 and Aβ42 fibrils form well-defined, discrete, individual 10-nm wide fibrils (Figure S2a,b). Application of the H/D protocol, followed by ESI-MS analysis of the Aβ40 and Aβ42 fibrils produced at pH 2.0, yielded a similar H/D time course to that obtained at pH 7.4. The spectra show two well-resolved peaks, corresponding to P_{pd} and P_{fd}, whereby the intensity of P_{fd} increases with time relative to that of P_{pd} (Figure S2c,d). H/D exchange is 4 orders of magnitude slower at pH 2.0 than at pH 7.4. Therefore, observation of a bimodal distribution at pH 2.0 is clear evidence that exchange occurs through the EX1 mechanism. We measured the fibril length distribution of the pH 2.0 fibrils using TEM (Figure S3) and then incorporated the measured value in recycling simulations. The experimental time course of the isotope exchange reaction was reproduced by a k_{off} of 1.5 s^{-1} for Aβ40 (green curve in Figure S2e) and a k_{off} of 0.5 $\times$ 10^{-2} s^{-1} for Aβ42 (green curve in Figure S2f). These values are close to the corresponding ones obtained at pH 7.4, 0.6 s^{-1} for Aβ40 (green curve in Figure 2e) and 1.0 $\times$ 10^{-2} s^{-1} for Aβ42 fibrils (green curve in Figure 2f), thereby indicating that association of fibrils into bundles did not greatly affect Aβ40 and Aβ42 k_{off} values.

To further validate our results, we considered that recycling is monitored under equilibrium conditions; thus, the rate of dissociation of protein molecules from the fibrils (ν_{off}) equals the rate of reincorporation of protein molecules into the fibrils (ν_{on}). Furthermore, our observation of P_{fd} species indicates that the rate of hydrogen exchange (ν_{ex}) is faster than ν_{on}. Thus, from the two aforementioned premises, it follows that $\nu_{off} = \nu_{on} < \nu_{ex}$. Applying experimental data to this equation, we calculated the maximum k_{off} value consistent with the observation of P_{fd} species (k_{off}^{max}) for each of our experimental conditions (Supporting discussion and Tables S1 and S2). The k_{off} values obtained from the simulations should be smaller than k_{off}^{max}, which is precisely the situation for all the conditions studied (Table S3, Figure S4). This proves that the H/D exchange experiments here described are indeed monitoring recycling within Aβ fibrils.

Our results show that Aβ fibrils continuously dissolve and reform, supporting a dynamic model for Aβ fibrils and providing evidence that Aβ fibril formation is not irreversible. These findings are consistent with a dynamical model based on competing aggregation and disaggregation processes proposed to interpret plaque morphology[16] and with studies on the interaction of Aβ42 and Aβ40 at different stages of aggregation.[17] Additionally, our data extend earlier work on fibril growth,[18] in which the authors proposed that only early interaction between fibrils and depositing Aβ was reversible, while becoming irreversibly associated to the fibril in a time-dependent manner.

We have quantitatively estimated the rate constants that determine fibril dissolution at pH 7.4: 0.6 s^{-1} for Aβ40 and 1.0 $\times$ 10^{-2} s^{-1} for Aβ42. These k_{off} values point to differences in fibril dissolution rates between Aβ40 and Aβ42 fibrils, being faster in the case of Aβ40 fibrils compared to Aβ42 fibrils. This reinforces the conclusions of other groups, who have reported that the biophysical behavior of Aβ40 is distinct from that of Aβ42.[19] Another important aspect of the k_{off} values obtained is that recycling occurs on time scales that are biologically relevant, not so fast as to be only thermodynamically important, and not so slow as to be kinetically irrelevant.

These results may have future implications for understanding how fibrils contribute to neurotoxicity in AD. Recently published data show that amyloid fibrils are a reservoir from which small Aβ oligomers are generated.[5] This finding would agree with our results on Aβ fibril recycling, assuming, first, that small oligomers, such as dimers and trimers, rather than monomers are involved in the recycling process and, second, that these oligomers are either intrinsically unprotected to exchange or in rapid dynamic equilibrium with the monomer.

Finally, our findings have important implications in the design of AD therapies. They highlight the importance of the Aβ variant used to test the efficiency of a given therapeutic strategy. Furthermore, they point to two possible therapeutic strategies: trapping the released Aβ species to promote subsequent

dissolution of the fibrils; and, if the released Aβ species are toxic,[5] blocking the fibril ends to prevent the release of Aβ molecules from the fibril. In fact, the H/D experiments used in this work to monitor molecular recycling stand as one possible means to test the efficacy of molecules that work by either of these two strategies.

■ ASSOCIATED CONTENT

Supporting Information. Materials and methods, discussion and tables related to the determination of k_{off}^{max}, figures reporting fibril length distributions, molecular recycling results for Aβ40 and Aβ42 amyloid fibrils produced at pH 2.0, additional simulation data and MS data, and complete ref 12c. This material is available free of charge via the Internet at http://pubs.acs.org.

■ AUTHOR INFORMATION

Corresponding Author
ernest.giralt@irbbarcelona.org; natalia.carulla@irbbarcelona.org

■ ACKNOWLEDGMENT

This work was supported by Program Grants from Fundació La Caixa, Fundació La Marató de TV3 (N.C. and E.G.), MICINN-FEDER BIO2008-00799 (E.G.), MICINN-FEDER SAF2009-07600 (N.C.), and Generalitat de Catalunya (XRB and Grup Consolidat).

■ REFERENCES

(1) Selkoe, D. J. *Ann. Intern. Med.* **2004**, *140*, 627–638.
(2) Hardy, J. A.; Higgins, G. A. *Science* **1992**, *256*, 184–185.
(3) Dickson, D. W.; Crystal, H. A.; Bevona, C.; Honer, W.; Vincent, I.; Davies, P. *Neurobiol. Aging* **1995**, *16*, 285–298.
(4) Haass, C.; Selkoe, D. J. *Nat. Rev. Mol. Cell. Biol.* **2007**, *8*, 101–112.
(5) Koffie, R. M.; Meyer-Luehmann, M.; Hashimoto, T.; Adams, K. W.; Mielke, M. L.; Garcia-Alloza, M.; Micheva, K. D.; Smith, S. J.; Kim, M. L.; Lee, V. M.; Hyman, B. T.; Spires-Jones, T. L. *Proc. Natl. Acad. Sci. U.S.A.* **2009**, *106*, 4012–4017.
(6) Kheterpal, I.; Zhou, S.; Cook, K. D.; Wetzel, R. *Proc. Natl. Acad. Sci. U.S.A.* **2000**, *97*, 13597–13601.
(7) Hoshino, M.; Katou, H.; Hagihara, Y.; Hasegawa, K.; Naiki, H.; Goto, Y. *Nat. Struct. Biol.* **2002**, *9*, 332–336.
(8) Luhrs, T.; Ritter, C.; Adrian, M.; Riek-Loher, D.; Bohrmann, B.; Dobeli, H.; Schubert, D.; Riek, R. *Proc. Natl. Acad. Sci. U.S.A.* **2005**, *102*, 17342–17347.
(9) Chetty, P. S.; Mayne, L.; Lund-Katz, S.; Stranz, D.; Englander, S. W.; Phillips, M. C. *Proc. Natl. Acad. Sci. U.S.A.* **2009**, *106*, 19005–19010.
(10) Carulla, N.; Caddy, G. L.; Hall, D. R.; Zurdo, J.; Gairi, M.; Feliz, M.; Giralt, E.; Robinson, C. V.; Dobson, C. M. *Nature* **2005**, *436*, 554–558.
(11) Guijarro, J. I.; Sunde, M.; Jones, J. A.; Campbell, I. D.; Dobson, C. M. *Proc. Natl. Acad. Sci. U.S.A.* **1998**, *95*, 4224–4228.
(12) (a) Iwatsubo, T.; Odaka, A.; Suzuki, N.; Mizusawa, H.; Nukina, N.; Ihara, Y. *Neuron* **1994**, *13*, 45–53. (b) Dahlgren, K. N.; Manelli, A. M.; Stine, W. B., Jr.; Baker, L. K.; Krafft, G. A.; LaDu, M. J. *J. Biol. Chem.* **2002**, *277*, 32046–32053. (c) McGowan, E.; et al. *Neuron* **2005**, *47*, 191–199. (d) Bentahir, M.; Nyabi, O.; Verhamme, J.; Tolia, A.; Horre, K.; Wiltfang, J.; Esselmann, H.; De Strooper, B. *J. Neurochem.* **2006**, *96*, 732–742. (e) Kumar-Singh, S.; Theuns, J.; Van Broeck, B.; Pirici, D.; Vennekens, K.; Corsmit, E.; Cruts, M.; Dermaut, B.; Wang, R.; Van Broeckhoven, C. *Hum. Mutat.* **2006**, *27*, 686–695.
(13) Carulla, N.; Zhou, M.; Arimon, M.; Gairi, M.; Giralt, E.; Robinson, C. V.; Dobson, C. M. *Proc. Natl. Acad. Sci. U.S.A.* **2009**, *106*, 7828–7833.
(14) Petkova, A. T.; Leapman, R. D.; Guo, Z.; Yau, W. M.; Mattson, M. P.; Tycko, R. *Science* **2005**, *307*, 262–265.
(15) Kayed, R.; Glabe, C. G. *Methods Enzymol.* **2006**, *413*, 326–344.
(16) Cruz, L.; Urbanc, B.; Buldyrev, S. V.; Christie, R.; Gomez-Isla, T.; Havlin, S.; McNamara, M.; Stanley, H. E.; Hyman, B. T. *Proc. Natl. Acad. Sci. U.S.A.* **1997**, *94*, 7612–7616.
(17) Jan, A.; Gokce, O.; Luthi-Carter, R.; Lashuel, H. A. *J. Biol. Chem.* **2008**, *283*, 28176–28189.
(18) Esler, W. P.; Stimson, E. R.; Jennings, J. M.; Vinters, H. V.; Ghilardi, J. R.; Lee, J. P.; Mantyh, P. W.; Maggio, J. E. *Biochemistry* **2000**, *39*, 6288–6295.
(19) (a) Jarrett, J. T.; Berger, E. P.; Lansbury, P. T., Jr. *Biochemistry* **1993**, *32*, 4693–4697. (b) Bitan, G.; Kirkitadze, M. D.; Lomakin, A.; Vollers, S. S.; Benedek, G. B.; Teplow, D. B. *Proc. Natl. Acad. Sci. U.S.A.* **2003**, *100*, 330–335. (c) Yan, Y.; Wang, C. *J. Mol. Biol.* **2006**, *364*, 853–62. (d) Olofsson, A.; Lindhagen-Persson, M.; Sauer-Eriksson, A. E.; Ohman, A. *Biochem. J.* **2007**, *404*, 63–70. (e) Bernstein, S. L.; Dupuis, N. F.; Lazo, N. D.; Wyttenbach, T.; Condron, M. M.; Bitan, G.; Teplow, D. B.; Shea, J.; Ruotolo, B. T.; Robinson, C. V.; Bowers, M. T. *Nat. Chem.* **2009**, *1*, 326–331.